E2E Throughput Maximisation in SWIPT aided Cooperative Communications with Time-Varying Channels

Yali Zheng[†], Jie Hu[†,*], Yizhe Zhao[†] and Kun Yang[‡,†]
[†]School of Information and Communication Engineering, University of Electronic Science and Technology of China, Chengdu, China, 611731
[‡]School of Computer Science and Electronic Engineering, University of Essex, Colchester, U.K., CO4 3SQ
[*]Corresponding author
Email: yalizheng@std.uestc.edu.cn, hujie@uestc.edu.cn, yzzhao@uestc.edu.cn, kunyang@essex.ac.uk

***Abstract*—Simultaneous wireless information and power transfer (SWIPT) has been considered as a promising technique to address energy shortage of communication devices deployed in Internet of Everything (IoE). In this paper, we consider a multi-relay aided cooperative communication network with SWIPT, where relay stations (RSs) receive RF signal from a source node (SN) for energy harvesting and information reception by power splitters. A single activated RS then decodes and forwards information to the destination using the harvested energy. Selective-decode-and-forward (S-DF) protocol is adopted, where the activated RS forwards only when information is correctly decoded. By considering time-varying channels, we maximise the end-to-end (E2E) throughput by jointly designing the transmit beamformers for both SN and RSs, optimising transmit power and power splitters for RSs, as well as the RS selection. The original formulated non-convex optimisation problem with coupled variables is solved by invoking an iterative algorithm. Numerical results demonstrate that our design with S-DF protocol outperforms that with the decode-and-forward (DF) protocol. Moreover, the impact of the imperfect channel state information (CSI) on the E2E throughput is also evaluated.**

***Index Terms*—SWIPT, cooperative communication, selective-decode-and-forward (S-DF), energy harvesting, time varying channels**

I. Introduction

Simultaneous wireless information and power transfer (SWIPT) [1], which integrates wireless power transfer (WPT) and wireless information transfer (WIT) in the same radio frequency (RF) bands, has emerged as a promising technique to satisfy the energy and communication demand of the increasing number of battery-powered or batteryless devices deployed in the Internet of Everything (IoE). Accordingly, SWIPT has received tremendous research interests in recent years. Many works focus on the coding [2] or modulation [3] design in the physical layer, as well as the resource allocation [4] and access control [5] in the medium-access-control (MAC) layer.

SWIPT also enables the flexible deployment of wireless powered relays for extending the coverage of IoE. Normally, DF protocol is one of the extensively adopted protocols in SWIPT-aided relays. For example, ignoring the energy consumption of decoding at relays, Ojo *et al.* [6] maximised energy efficiency in a SWIPT aided decode-and-forward (DF) cooperative system with a single relay by optimising source's transmit power, relay's power splitting and energy consumed factors.

However, in a conventional DF protocol [7], relays may forward error information since they do not check transmission errors during their information decoding. Recently, a novel selective-decode-and-forward (S-DF) protocol [8] was proposed for overcoming the drawbacks of the conventional DF protocol and was considered for different communication scenarios. Specifically, relays are activated for forwarding information decoded correctly with those having errors discarded. For example, Bouteggui *et. al* [9] maximised the end-to-end (E2E) throughput by jointly designing the antennas and transmission paths selection strategy in S-DF aided cooperative communications. The symbol-error-probability (SEP) of the S-DF protocol was analysed in a multi-relay aided satellite-terrestrial wireless network [10]. These works demonstrate the advantage of the S-DF protocol over the DF counterpart. Additionally, the S-DF protocol saves transmission energy by only forwarding the correctly decoded information. Babaei *et. al* [11] derived the bit error probability by analysing power splitting and time switching protocols in SWIPT-aided cooperative communications including a single relay. However, quite few works leverage the energy-saving property of the S-DF protocol in SWIPT-aided system.

Against this background, we aim to utilize the maximize the E2E throughput in SWIPT-aided cooperative communications over time-varying channels. Our novel contributions are summarised as follows:

- We consider a SWIPT aided cooperative communication network with multiple battery-powered relays adopting S-DF protocol. Each relay receives the downlink RF signals transmitted by a source, while simultaneously harvesting energy and decoding information by their power splitters. The relay forwards only in case of correctly decoding the information; otherwise, it only harvests and stores energy for the future transmission.
- By considering the decoding energy consumption, transmit beamformers for the source and the relays, transmit power and power splitters for the relays and relay selection are jointly optimised.

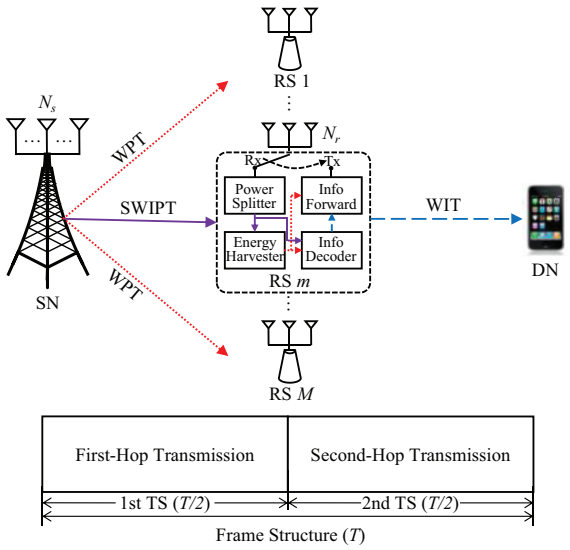

Fig. 1. System model of the downlink SWIPT-aided cooperative communication network.

- Numerical results demonstrate our joint design with the S-DF protocol outperforms that with the classic DF counterpart over time-varying channels. The impact of partial channel state information (CSI) knowledge on the E2E throughput performance is also evaluated by assuming that the perfect CSI of only the first transmission frame in a single transmission cycle is available.

The rest of the paper is organised as follows. The system model and the problem formulation are described in Section II and III, respectively. After proposing our joint design in Section IV, numerical results are presented in Section V. Finally, we conclude our paper in Section VI.

Notations: In this paper, we use the letter a to represent a scalar. The uppercase and lowercase boldface letters, $\mathbf{A}$ and $\mathbf{a}$, denote matrices and vectors, respectively. The calligraphic letter $\mathcal{A}$ represents a set. $\mathbf{A}^\dagger$ is the conjugate transpose of $\mathbf{A}$. $\mathrm{Tr}(\mathbf{A})$ is the trace of $\mathbf{A}$. Finally, $|\mathcal{A}|$ is the cardinality of $\mathcal{A}$.

II. System Model

A. Network Model

We consider a downlink SWIPT-aided cooperative communication network, consisting of a single source node (SN), a set of M cooperative relay stations (RSs), and a single destination node (DN), as illustrated in Fig. 1. We also assume that the RSs follow a classic "save-then-transmit" protocol [12]. Accordingly, to complete an E2E WIT, the RF signal experiences a two-hop transmission. In the 1st-hop, the SN equipped with N_s transmit antennas (TAs) propagates the RF signals to M RSs. However, we assume that only one of the M RSs is activated to decode the received signal and harvest energy, while the rest $(M-1)$ RSs receive the RF signal only for energy harvesting in the 1st-hop. In the 2nd-hop, the activated RS m forwards the correctly decoded information to the single-antenna DN and the rest $(M-1)$ RSs remain idle. Therefore, the activated RS m with N_r antennas operating on the half-duplex (HD) mode have a pair of functions:

- *Signal reception:* The RS m divides the received RF signals from SN by power splitters, i.e., a part for energy harvesting and the other for information decoding. The harvested energy is stored into the equipped batteries as the RS m's only energy source for both information decoding & forwarding;
- *Information forwarding:* By invoking the S-DF protocol, the RS m forwards the information transmitted by the SN to the DN only when the information is decoded correctly.

We assume that a single transmission cycle consists of L transmission frames. By adopting the time-division-multiple-access (TDMA) protocol, a complete transmission frame having a time duration of T is composed of two equal time slots (TSs), to complete the 1st-hop and 2nd-hop transmission, respectively, as shown in Fig. 1.

B. Channel Model

The time-varying channel model [13] is considered in this paper. As discussed in Section II-A, the downlink E2E WIT is completed via two-hop transmissions. In the 1st-hop transmission, the channel matrix $\mathbf{H}_{s,m}(l) \in \mathbb{C}^{N_r \times N_s}$ represents the normalised downlink channel fading coefficients from the SN's N_s TAs to RS m's N_r antennas during the l-th transmission frame, $l = 2, 3, \cdots, L$, which is formulated as

$$\begin{aligned}\mathbf{H}_{s,m}(l) =& \lambda_{s,m}\mathbf{H}_{s,m}(l-1) + \Delta\mathbf{H}_{s,m}(l),\\ =& \lambda_{s,m}^{l-1}\mathbf{H}_{s,m}(1) + \sum_{l'=2}^{l}\lambda_{s,m}^{l-l'}\Delta\mathbf{H}_{s,m}(l'),\end{aligned} \tag{1}$$

where $0 \le \lambda_{s,m} \le 1$ represents the temporal fading coefficient. The elements of $\Delta\mathbf{H}_{s,m}$ are i.i.d. $\mathcal{CN}(0, (1-\lambda_{s,m}^2)\sigma_{h,sm}^2)$, where $\sigma_{h,sm}^2$ is the channel variance.

Similarly, in the 2nd-hop transmission, the normalised fading coefficients of the downlink channel from the RS m's N_r antennas to the single-antenna DN during the l-th time slot are collected in a vector $\mathbf{h}_{m,d}(l) \in \mathbb{C}^{1\times N_r}$, which is expressed as

$$\mathbf{h}_{m,d}(l) = \lambda_{m,d}^{l-1}\mathbf{h}_{m,d}(1) + \sum_{l'=2}^{l}\lambda_{m,d}^{l-l'}\Delta\mathbf{h}_{m,d}(l'), \tag{2}$$

where $0 \le \lambda_{m,d} \le 1$ is the temporal fading coefficient, and the elements of $\Delta\mathbf{h}_{m,d}$ are i.i.d. $\mathcal{CN}(0, (1-\lambda_{m,d}^2)\sigma_{h,md}^2)$, where $\sigma_{h,md}^2$ is the channel variance.

Furthermore, $\Omega_{s,m}$ and $\Omega_{m,d}$ represent the large-scale path-loss between the SN and the RS m and that between RS m and the DN, respectively.

III. Problem Formulation

A. SWIPT in the 1st-Hop Transmission

Without loss of generality, during the 1st time slot of the l-th transmission frame, the SN broadcasts a modulated RF signal $x(l)$ which has a zero mean and a variance of $\mathbb{E}[x(l)x^\dagger(l)] = 1$ to all RSs. The received RF signal at the RS m can be expressed

as

$$\mathbf{y}_m(l) = \lambda_{s,m}^{l-1}\sqrt{P_s(l)/\Omega_{s,m}}\mathbf{H}_{s,m}(1)\mathbf{w}_s(l)x(l) + \underbrace{\sum_{l'=2}^{l}\lambda_{s,m}^{l-l'}\sqrt{P_s(l)/\Omega_{s,m}}\Delta\mathbf{H}_{s,m}(l')\mathbf{w}_s(l)x(l) + \mathbf{n}_m(l)}_{\text{Channel error } \mathbf{y}_{ce}(l)}, \quad (3)$$

where $P_s(l)$ is the transmit power of the SN and $\mathbf{y}_{ce}(l)$ represents the channel error. Notice that we have $\mathbf{y}_{ce}(l) = \mathbf{0}_{N_r\times 1}$ for $l = 1$ owing to the assumption of perfect CSI in the 1st time slot. Moreover, $\mathbf{w}_s(l) \in \mathbb{C}^{N_s\times 1}$ is the normalised transmit beamformer satisfying $\mathrm{Tr}\left(\mathbf{w}_s(l)\mathbf{w}_s^{\dagger}(l)\right) \leq 1$. The elements of the $N_r \times 1$ AWGN vector $\mathbf{n}_m(l)$ obey the complex Gaussian distribution having a zero mean and a variance of σ_m^2.

A maximal ratio combiner $\mathbf{w}_{c,m}$ is invoked for combining the signal $\mathbf{y}_m(l)$ received by the RS m's N_r antennas. Accordingly, the power of the combined signal $\mathbf{w}_{c,m}\mathbf{y}_m(l)$ is expressed as

$$P_{\mathrm{c,m}}(l) = \lambda_{s,m}^{2(l-1)}P_s(l)\mathrm{Tr}\left(\mathbf{H}_{s,m}(1)\mathbf{w}_s(l)\mathbf{w}_s^{\dagger}(l)\mathbf{H}_{s,m}^{\dagger}(1)\right)/\Omega_{s,m} + \left(1-\lambda_{s,m}^{2(l-1)}\right)P_s(l)\sigma_{h,sm}^2/\Omega_{s,m} + \sigma_m^2. \quad (4)$$

Since RSs divide the received RF signal by power splitters, we denote the RS m's power-splitting factors over L transmission frames as $\boldsymbol{\rho}_m = \{\rho_m(l)|l = 1,\cdots,L\}$, for $m = 1,\cdots,M$, where $0 \leq \rho_m(l) \leq 1$. The portion $\rho_m(l)$ of the combined signal's power $P_{\mathrm{c,m}}(l)$ is exploited for the energy harvesting. Therefore, the energy converted by a linear energy harvester of the RS m during the l-th transmission frame is formulated as $E_m(l) = \frac{T}{2}\left(k\rho_m(l)P_{\mathrm{c,m}}(l)\right)$, where k is the conversion efficiency. The other fraction $(1-\rho_m(l))$ of $P_{\mathrm{c,m}}(l)$ is exploited for the information decoding.

Theorem 1: The signal-to-noise-ratio (SNR) $\gamma_m(l)$ of the combined signal for the information decoding is formulated as Eq. (5) on the next page, where σ_{cov}^2 is the power of the Gaussian distributed noise incurred by the imperfect passband-to-baseband converter.

Proof: Please refer to Appendix A for detailed proof. ■

Since only a single RS is activated for decoding and forwarding during a single transmission frame, RSs activation can be denoted as a binary indicator vector $\boldsymbol{\alpha} = \{\alpha_m|m = 1,\cdots,M\}$ obeying the following constraints:

$$\sum_{m=1}^{M}\alpha_m \leq 1, \quad (6)$$

$$\alpha_m \in \{0,1\}, \forall m = 1,\cdots,M, \quad (7)$$

where $\alpha_m = 1$ represents that the RS m is activated to decode and relay the information; otherwise, $\alpha_m = 0$. Therefore, the throughput $R_r(l)$ for information decoding in the 1st-hop transmission during the l-th transmission frame can be expressed as

$$R_r(l) = \frac{T}{2}\sum_{m=1}^{M}\alpha_m \underbrace{\log(1+\gamma_m(l))}_{\text{Information rate } r_m(l)}, \quad (8)$$

where $r_m(l)$ denotes the information rate received by the RS m's information decoder during the l-th transmission frame.

Furthermore, we assume that when the SNR $\gamma_m(l)$ reaches a predefined threshold $\gamma_{m,th}$, the RS m decodes information with no error, i.e., $\gamma_m(l) \geq \gamma_{m,th}$. Additionally, the binary indicator vector $\boldsymbol{\beta}_m = \{\beta_m(l)|l = 1,\cdots,L\}$, $m = 1,\cdots,M$ is defined for identifying the correct/false decoding over L transmission frames, where $\beta_m(l) = 1$ indicates that the RS m correctly decodes during the l-th transmission frame; otherwise, $\beta_m(l) = 0$. Therefore, the RS m's residual energy at the end of the l-th transmission frame can be formulated as

$$Q_m(l) = Q_m(l-1) + E_m(l) - \frac{T}{2}\alpha_m\left[\varphi_m(l) + \beta_m(l)P_m(l)\right], \quad (9)$$

where $Q_m(l-1)$ represents the RS m's residual energy after the $(l-1)$-th transmission frame; the transmit power of the RS m is denoted as $\mathbf{P}_m = \{P_m(l)|l = 1,\cdots,L\}$; and $\varphi_m(l) = a\left(2^{r_m(l)}-1\right)$[W] represents the information decoding power [14], where a represents the decoding cost factor.

B. WIT in the 2nd-Hop Transmission

In the 2nd-hop transmission, the discrete received RF signal $y_{m,d}(l)$ at the DN relayed by the RS m can be expressed as

$$y_{m,d}(l) = \sqrt{\frac{P_m(l)}{\Omega_{m,d}}}\mathbf{h}_{m,d}(l)\mathbf{w}_m(l)x_m(l) + n_d(l), \quad (10)$$

where $x_m(l)$ is the modulated RF signal having a zero mean and variance of $\mathbb{E}[x_m(l)x_m^{\dagger}(l)] = 1$; $n_d(l)$ is a Gaussian distributed complex noise having a zero mean and a variance of σ_d^2; and $\mathbf{w}_m(l) \in \mathbb{C}^{N_r\times 1}$ denotes the transmit beamformer of the RS m, which can be formulated as $\mathbf{w}_m(l) = \mathbf{h}_{m,d}^{\dagger}(l)/\parallel\mathbf{h}_{m,d}(l)\parallel$ by adopting the classic MRC method [15].

According to Appendix A, the SNR of $y_{m,d}(l)$ is formulated as

$$\gamma_{m,d}(l) = \frac{\lambda_{m,d}^{2(l-1)}P_m(l)\parallel\mathbf{h}_{m,d}(1)\parallel^2}{\left(1-\lambda_{m,d}^{2(l-1)}\right)\sigma_{h,md}^2P_m(l) + \Omega_{m,d}\sigma_d^2}. \quad (11)$$

Therefore, the throughput in the 2nd-hop transmission during the l-th transmission frame can be formulated as $R_d(l) = \frac{T}{2}\sum_{m=1}^{M}\alpha_m\beta_m(l)\log(1+\gamma_{m,d}(l))$. Now, the E2E throughput from the SN to the DN during a complete transmission cycle with L frames can be expressed as

$$R_{e2e} = \sum_{l=1}^{L}\min\{R_r(l), R_d(l)\}. \quad (12)$$

C. Downlink Sum-Throughput Maximisation

Our joint resource scheduling design can be formulated as the following E2E throughput optimisation problem:

$$\text{(P1)}: \max_{\mathbf{w}_s(l),\boldsymbol{\rho}_m,\mathbf{P}_m,\boldsymbol{\alpha}} R_{e2e}, \quad (13)$$

$$\text{s. t. } \mathrm{Tr}\left(\mathbf{w}_s(l)\mathbf{w}_s^{\dagger}(l)\right) \leq 1, \forall l = 1,\cdots,L, \quad (13a)$$

$$0 \leq \rho_m(l) \leq 1, \forall m = 1,\cdots,M, \forall l = 1,\cdots,L, \quad (13b)$$

$$P_m(l) \geq 0, \forall m = 1,\cdots,M, \forall l = 1,\cdots,L, \quad (13c)$$

$$Q_m(l) \geq 0, \forall m = 1,\cdots,M, \forall l = 1,\cdots,L, \quad (13d)$$

$$(6) \text{ and } (7).$$

(P1) aims for maximising the downlink E2E throughput over L transmission frames by optimising the SN's transmit beamformer $\mathbf{w}_s(l), l = 1,\cdots,L$, the RSs' signal splitter $\boldsymbol{\rho}_m$, transmit

$$\gamma_m(l) = \frac{(1-\rho_m(l))\lambda_{s,m}^{2(l-1)} P_s(l) \mathrm{Tr}\left(\mathbf{H}_{s,m}(1)\mathbf{w}_s(l)\mathbf{w}_s^{\dagger}(l)\mathbf{H}_{s,m}^{\dagger}(1)\right)}{(1-\rho_m(l))\left(1-\lambda_{s,m}^{2(l-1)}\right) P_s(l)\sigma_{h,sm}^2 + \Omega_{s,m}\left[(1-\rho_m(l))\,\sigma_m^2 + \sigma_{cov}^2\right]} \tag{5}$$

power $\mathbf{P}_m$, as well as the RSs' binary activation indicator vector $\boldsymbol{\alpha}$. Constraint (13a) ensures normalised $\mathbf{w}_s(l)$. Constraints (13b)-(13d) limit the range of the RSs' signal splitter, transmit power, and residual energy, respectively. Constraints (6) and (7) have been defined in Section III-A.

IV. Joint Optimisation algorithm for E2E Throughput Maximization

Due to the coupled optimisation variables $\{\mathbf{w}_s(l), \boldsymbol{\rho}_m, \mathbf{P}_m\}$, as well as the discrete vectors $\{\boldsymbol{\alpha}, \boldsymbol{\beta}_m\}$, (P1) is non-convex. In this section, we first transform (P1) into a sub-problem (P2) by giving fixed $\{\boldsymbol{\alpha}, \boldsymbol{\beta}_m\}$ and further decouple it into three convex sub-problems, which aim for optimising $\mathbf{w}_s(l)$, $\boldsymbol{\rho}_m$ and $\mathbf{P}_m$, respectively, by fixing other optimisation variables. (P2) is solved by iteratively solving the three sub-problems until it converges. Finally, the proposed join design is obtained by traversing $\boldsymbol{\alpha}$ and $\boldsymbol{\beta}_m$.

Firstly, we assume that the RS m' is activated, i.e., $\alpha_{m'} = 1$, and $\boldsymbol{\beta}_{m'}$ is fixed. We define a pair of non-overlapping sets $\mathcal{L}_{m',k}^{+}$ and $\mathcal{L}_{m',k}^{-}$ as the indices of transmission frames, satisfing $\mathcal{L}_{m',k}^{+} + \mathcal{L}_{m',k}^{-} = \{1, 2, \cdots, L\}$. We have $\mathcal{L}_{m',k}^{+} = \{l \mid \beta_{m'}(l) = 1\}$ and $\mathcal{L}_{m',k}^{-} = \{l \mid \beta_{m'}(l) = 0\}$, for $\forall l = \{1, 2, \cdots, L\}$. Then, (P1) can be reformulated as

$$\text{(P2)}: \max_{\mathbf{w}_s(l), \boldsymbol{\rho}_{m'}, \mathbf{P}_{m'}} R_{e2e}, \tag{14}$$

$$\text{s. t. } \gamma_{m'}(l) \geq \gamma_{m',th}, \forall l \in \mathcal{L}_{m',k}^{+}, \tag{14a}$$

$$\gamma_{m'}(l) < \gamma_{m',th}, \forall l \in \mathcal{L}_{m',k}^{-}, \tag{14b}$$

$$\text{(13a), (13b), (13c), and (13d).}$$

When $\{\boldsymbol{\rho}_{m'}, \mathbf{P}_{m'}\}$ is given and fixed, by letting $\mathbf{W}_s(l) = \mathbf{w}_s(l)\mathbf{w}_s^{\dagger}(l)$, and by relaxing the rank-one constraint on the positive semi-definite covariance matrix $\mathbf{W}_s(l)$, (P2) can be reformulated as the following covariance matrix design:

$$\text{(P3)}: \max_{\mathbf{W}_s(l)} R_{e2e} \tag{15}$$

$$\text{s. t. (13a), (13d), (14a) and (14b).}$$

Since the optimal solution to (P3) is obtained when the RS m' receives the downlink signal with a maximum SNR, (P3) can be equivalently reformulated as the following semi-definite programming problem (P3-1).

$$\text{(P3-1)}: \max_{\mathbf{W}_s(l)} \mathrm{Tr}\left(\mathbf{H}_{s,m}(1)\mathbf{W}_s(l)\mathbf{H}_{s,m}^{\dagger}(1)\right) \tag{16}$$

$$\text{s. t. } \mathrm{Tr}\left(\mathbf{W}_s(l)\right) \leq 1.$$

Since we assume that only the CSI in the first transmission frame is available, we have $\mathbf{W}_s(1) = \cdots = \mathbf{W}_s(L)$.

Given fixed $\{\mathbf{W}_s(l), \mathbf{P}_{m'}\}$, (P2) can be reformulated as

$$\text{(P4)}: \max_{\boldsymbol{\rho}_{m'}} R_{e2e} \tag{17}$$

$$\text{s. t. (13b), (13d), (14a) and (14b).}$$

Algorithm 1 An iterative algorithm based joint design for solving (P2)

Input: All the physical/MAC layer parameters, such as M, N_s, N_r, $\Omega_{s,m}$, $\Omega_{m,d}$, L, $\{(\mathbf{H}_{s,m}(l), \mathbf{h}_{m,d}(l)) | l = 1, \cdots, L\}$, $\gamma_{m,th}$, $\sigma_{h,sm}^2$ and $\sigma_{h,md}^2$. RSs' binary activation indicator vector $\boldsymbol{\alpha}$ and decoding indicator vector $\boldsymbol{\beta}_{m'}$. Difference threshold ϵ.

Output: Solution $\{\mathbf{W}_s^*(l), \mathbf{P}_{m'}^*, \boldsymbol{\rho}_{m'}^*\}$. E2E throughput R_{e2e}^*.

1: Initialise $\boldsymbol{\rho}_{m',(0)} \leftarrow [\rho_{m'}(l) \leftarrow 0.5]_{1\times L}$, $\mathbf{P}_{m',(0)} \leftarrow [P_{m'}(l) \leftarrow 10^{-4}(\mathrm{W})]_{1\times L}$;
2: Initialise $R_{e2e,cur} \leftarrow 0$, $R_{e2e,pre} \leftarrow -2\epsilon$ and iteration number $i \leftarrow 0$;
3: **while** $|R_{e2e,cur} - R_{e2e,pre}| > \epsilon$ **do**
4: $\quad R_{e2e,pre} \leftarrow R_{e2e,cur}$;
5: $\quad$ Update $\mathbf{W}_{s,(i+1)}(l) \leftarrow \mathbf{W}_s^*(l)$ by solving (P3-1) after substituting $\{\boldsymbol{\rho}_{m',(i)}, \mathbf{P}_{m',(i)}\}$ into it;
6: $\quad$ Update $\boldsymbol{\rho}_{m',(i+1)} \leftarrow \boldsymbol{\rho}_{m'}^*$ by solving (P4) after substituting $\{\mathbf{W}_{s,(i+1)}(l), \mathbf{P}_{m',(i)}\}$ into it;
7: $\quad$ Update $\mathbf{P}_{m',(i+1)} \leftarrow \mathbf{P}_{m'}^*$ and $R_{e2e,cur} \leftarrow R_{e2e}^*$ by solving (P5) after substituting $\{\mathbf{W}_{s,(i+1)}(l), \boldsymbol{\rho}_{m',(i+1)}\}$ into it;
8: $\quad$ Update $i \leftarrow i + 1$;
9: **end while**
10: **return** $\{\mathbf{W}_s^*(l), \boldsymbol{\rho}_{m'}^*, \mathbf{P}_{m'}^*\} \leftarrow \{\mathbf{W}_{s,(i)}(l), \boldsymbol{\rho}_{m',(i)}, \mathbf{P}_{m',(i)}\}$ and $R_{e2e}^* \leftarrow R_{e2e,cur}$.

Given fixed $\{\mathbf{W}_s(l), \boldsymbol{\rho}_{m'}\}$, (P2) can be reformulated as

$$\text{(P5)}: \max_{\mathbf{P}_{m'}} R_{e2e} \tag{18}$$

$$\text{s. t. (13c), (13d), (14a) and (14b).}$$

Now, (P3-1), (P4) and (P5) are all convex problems, which can be solved by any convex optimisation tool. Therefore, we can iteratively obtain the optimal solution to (P2) by adopting an iterative algorithm. The joint design to (P1) can be further obtained by traversing the binary indicator vectors $\boldsymbol{\alpha}$ and $\boldsymbol{\beta}_m$. The pseudo code of the proposed iterative design for solving (P2) is detailed in Algorithm 1, which has the following main steps:

- *Step 1*: Initialise $\boldsymbol{\rho}_{m',(0)}$ by equally splitting the received RF signal, i.e., $\rho_{m'}(l) = 0.5$, while initialising transmit power $P_{m'}(l)$ of $RS_{m'}$ during l-th transmission frame as 10^{-4} W, as shown in Line 1 of Algorithm 1.
- *Step 2*: By exploiting the optimal solution $\{\mathbf{W}_{s,(i)}(l), \boldsymbol{\rho}_{m',(i)}, \mathbf{P}_{m',(i)}\}$ obtained in the last iteration, we can sequentially update them as $\{\mathbf{W}_{s,(i+1)}(l), \boldsymbol{\rho}_{m',(i+1)}, \mathbf{P}_{m',(i+1)}\}$ by solving (P3-1), (P4) and (P5), respectively, as characterised in Lines 4-8 of Algorithm 1.
- *Step 3*: If difference between the E2E throughput $R_{e2e,cur}$ obtained in the current iteration and $R_{e2e,pre}$ in the last one is higher than the pre-defined threshold ϵ, we repeat Step 2, as shown in Line 3 of Algorithm 1. Otherwise, $\{\mathbf{W}_{s,(i)}(l), \boldsymbol{\rho}_{m',(i)}, \mathbf{P}_{m',(i)}\}$ and $R_{e2e,cur}$ are the outputs, as shown in Line 10 of Algorithm 1.

Convergence and complexity analysis: R_{e2e} is nondecreasing after each iteration in Algorithm 1. Since a continuous function has an upper-bound in a closed interval, R_{e2e} has a upper-bound with respect to the continuous inputs $\{\mathbf{W}_s(l), \boldsymbol{\rho}_{m'}, \mathbf{P}_{m'}\}$. Therefore, the proposed algorithm is guaranteed to converge.

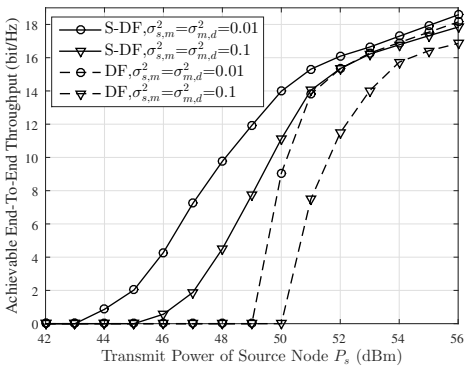

Fig. 2. Impact of transmit power of the SN on the E2E throughput.

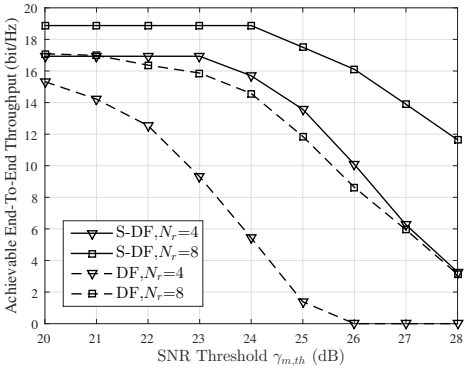

Fig. 3. Impact of decoding SNR threshold on the E2E throughput.

The complexity of the interior point method based convex optimisation tool for solving the three subproblems (P3-1), (P4) and (P5) is $O(x)^{3.5}$ [16], where x is the number of the variables. Therefore, every iteration can be completed in polynomial time. Since Algorithm 1 definitely converges after a finite number of iterations, the complexity of Algorithm 1 is polynomial.

Rank-1 recovery: After the convergence of Algorithm 1, the vector $\mathbf{w}_s^*(l)$ can be approximated by Gaussian randomisation methodology [17].

V. Numerical Results

In this section, we characterise our E2E throughput performance under different system settings. Specifically, in this section, the channel path-loss $\Omega_{s,m}$ in the 1st-hop transmission and $\Omega_{m,d}$ in the 2nd-hop channel can be formulated as $\Omega = \Omega_0 \cdot \left(\frac{d}{d_0}\right)^{\alpha}$ for $(\Omega, d) = \{(\Omega_{s,m}, d_{s,m}), (\Omega_{m,d}, d_{m,d})\}$. Simulation parameters in both physical and MAC layers are set as follows, unless otherwise mentioned. In our simulations, we have $P_s = 50$ dBm, $N_s = L = M = 4$, $N_r = 2$, $\sigma_m^2 = \sigma_d^2 = -60$ dBm, $\Omega_0 = 30$ dB, $d_0 = 1$ m, $\sigma_{h,sm}^2 = \sigma_{h,md}^2 = 0.01$, $\lambda_{s,m} = \lambda_{m,d} = 0.99$, $\gamma_{m,th} = 22$ dB, $k = 0.8$, $d_{s,m} = d_{m,d} = [2, 4]$ m and $a = 10^{-3}$ [14].

We consider the Rayleigh fading in the 1st- and 2nd-hop channels, owing to the complicated environment between the SN and the DN. RSs are randomly distributed within the distance range. All the results are obtained by averaging the randomness incurred by the Rayleigh fading.

A. Transmit Power

We firstly investigate the impact of the SN's transmit power on the downlink E2E throughput with S-DF and DF protocols, as shown in Fig. 2. Note that in the DF protocol, RSs decode and forward all received signals transmitted by the SN, which may result in invalid information forwarding. Observe from Fig. 2 that when we increase the transmit power of the SN, the downlink E2E throughput is substantially increased from zero. This is because, when the SN's transmit power is low, RSs fail to decode correctly. As we initially increase the SN's transmit power, the RSs may gain more energy and higher SNR from the downlink SWIPT. Therefore, they obtain a higher successful decoding probability, and harvest a higher amount of energy for powering their own downlink WIT. Observe from Fig. 2 that our system with the S-DF protocol outperforms that with the DF protocol, since RSs in the DF protocol may waste their energy to execute invalid WIT. Furthermore, the E2E throughput reduces as we increase channel variances $\sigma_{s,m}^2$ and $\sigma_{m,d}^2$ from 0.01 to 0.1.

B. Decoding SNR Threshold

We then investigate the impact of decoding SNR threshold on the E2E throughput, by fixing $\sigma_{h,sm}^2$ and $\sigma_{h,md}^2$ at 0.1. Observe from Fig. 3 that the downlink E2E throughput reduces as we increase the decoding SNR threshold $\gamma_{m,th}$. This is because the increasing SNR threshold makes the successfully decoding more challenging, resulting in a decreasing throughput. However, as we continuously increase the threshold, a very high decoding SNR threshold may cause the consequence that RSs cannot perform WIT in the system with S-DF protocol (or carry out valid WIT in the system with DF protocol). Hence, the E2E throughput drops to zero, as shown in Fig. 3. Furthermore, when we increase the number of the RSs' antennas from $N_r = 4$ to 8, the transmission performance of RSs is significantly improved.

C. Transmission Frames

Fig. 4 depicts the impact of the number of transmission frames L on the average downlink E2E throughput per transmission frame. Observe from Fig. 4 that when the SN's transmit power is high, such as $P = 50$ dBm, the throughput decreases as the L increases. This is because the channel interference increases due to the channel errors, resulting in the decrease of E2E throughput. When the SN's transmit power is set to $P = 47$ dBm and 40 dBm, the throughput first increase and then decrease as the number of transmission frames increase. This is because RSs need enough transmission frames to harvest energy for powering its own decoding and forwarding. However, when the number of frames continuously increase, the throughput performance reduces.

VI. Conclusion

We studied a SWIPT-aided cooperative communication network adopting the S-DF protocol. Considering time-varying channels, we maximise the E2E throughput by jointly designing the relay selection, power allocation, transmit beamforming and signal splitting. The iterative joint design is proposed

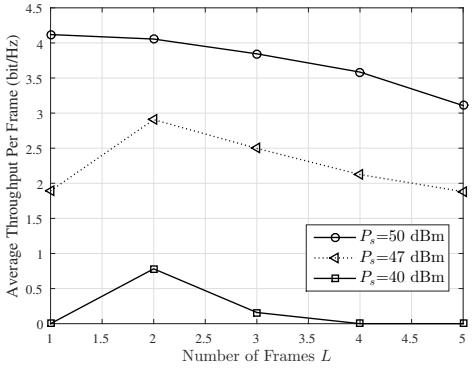

Fig. 4. Impact of the number of the transmission frames on the average E2E throughput per transmission frame.

for solving the original formulated non-convex optimisation problems. Numerical results validate the superiority of the E2E throughput achieved by the S-DF protocol over the traditional DF protocol. Furthermore, we also evaluate the impact of the imperfect CSI on the E2E throughput.

Appendix A
Proof of Theorem. 1

By considering imperfect CSI in a system, where a source transmits the signal S to a destination, we denote the signal received by the destination as Y, which can be formulated as

$$Y = FS + N = (\bar{F} + \hat{F})S + N, \tag{19}$$

where S is the source information having a variance of σ_s^2. $\bar{F}$ is the estimated channel coefficient and $\hat{F}$ is the channel coefficient error following a Gaussian distribution having a variance of σ_F^2. Moreover, N is the Gaussian distributed complex noise having a variance of σ_N^2. Therefore, the mutual information between S and Y is formulated as

$$I(Y;S) = h(S) - h(S|Y), \tag{20}$$

where $h(\cdot)$ represents the entropy function. Since the conditional entropy satisfies $h(S|Y = y) = h(S - ay|Y = y)$, we have $h(S|Y) = h(S - aY|Y)$, where a is an arbitrary real number. Given the fact that $h(S - aY|Y) \leq h(S - aY)$, we have $h(S|Y) \leq h(S - aY) \leq \frac{1}{2}\ln(2\pi e Var(S - aY))$. When $Var(S - aY)$ achieves its minimum, we have

$$\begin{aligned} a &= \frac{\mathbb{E}[SY]}{\mathbb{E}[Y^2]} = \frac{\bar{F}\sigma_S^2}{\bar{F}^2\sigma_S^2 + \sigma_S^2\sigma_F^2 + \sigma_N^2}, \\ Var(S - aY) &= \frac{\sigma_S^4\sigma_F^2 + \sigma_N^2\sigma_S^2}{\bar{F}^2\sigma_S^2 + \sigma_S^2\sigma_F^2 + \sigma_N^2}. \end{aligned} \tag{21}$$

Therefore, the conditional entropy satisfies $h(S|Y) \leq \frac{1}{2}\ln(2\pi e \frac{\sigma_S^4\sigma_F^2 + \sigma_N^2\sigma_S^2}{\bar{F}^2\sigma_S^2 + \sigma_S^2\sigma_F^2 + \sigma_N^2})$. The lower bound of the mutual information satisfies

$$\begin{aligned} I(S;Y) \geq& \frac{1}{2}\ln(2\pi e\sigma_s^2) - \frac{1}{2}\ln(2\pi e \frac{\sigma_S^4\sigma_F^2 + \sigma_N^2\sigma_S^2}{\bar{F}^2\sigma_S^2 + \sigma_S^2\sigma_F^2 + \sigma_N^2}) \\ =& \frac{1}{2}\ln(1 + \frac{\bar{F}^2\sigma_S^2}{\sigma_S^2\sigma_F^2 + \sigma_N^2}). \end{aligned} \tag{22}$$

When the equation holds, the SNR is formulated as

$$\gamma = \frac{\bar{F}^2\sigma_S^2}{\sigma_S^2\sigma_F^2 + \sigma_N^2}. \tag{23}$$

According to the received RF signal at the RS_m in Eq. (3), its SNR is then formulated as Eq.(5). *Theorem 1* is proved.

Acknowledgment

This work was supported by the National Natural Science Foundation of China (No. 62132004, 61971102, 62201123), MOST Major Research and Development Project (No. 2021YFB2900204), Sichuan Science and Technology Program (No. 2022YFH0022), UESTC Yangtze Delta Region Research Institute-Quzhou (No. 2021D003).

References

[1] J. Hu, Y. Zhao, and K. Yang, "Modulation and coding design for simultaneous wireless information and power transfer," *IEEE Commun. Mag.*, vol. 57, no. 5, pp. 124–130, May 2019.

[2] J. Hu, M. Li, K. Yang, S. X. Ng, and K. Wong, "Unary coding controlled simultaneous wireless information and power transfer," *IEEE Trans. Wireless Commun.*, vol. 19, no. 1, pp. 637–649, 2020.

[3] Y. Zhao, J. Hu, Z. Ding, and K. Yang, "Joint interleaver and modulation design for multi-user SWIPT-NOMA," *IEEE Trans. Commun.*, vol. 67, no. 10, pp. 7288–7301, 2019.

[4] G. A. Ropokis and P. S. Bithas, "Wireless powered relay networks: Rate optimal and power consumption-aware WPT/SWIPT," *IEEE Trans. Veh. Technol.*, vol. 71, no. 8, pp. 8574–8590, 2022.

[5] Y. Zhao, J. Hu, Y. Diao, Q. Yu, and K. Yang, "Modelling and performance analysis of wireless LAN enabled by RF energy transfer," *IEEE Trans. Commun.*, vol. 66, no. 11, pp. 5756–5772, 2018.

[6] F. K. Ojo and M. F. Mohd Salleh, "Energy efficiency optimization for SWIPT-enabled cooperative relay networks in the presence of interfering transmitter," *IEEE Commun. Letters*, vol. 23, no. 10, pp. 1806–1810, 2019.

[7] Y. Shim, W. Shin, and M. Vaezi, "Relay power control for in-band full-duplex decode-and-forward relay networks over static and time-varying channels," *IEEE Systems Journal*, vol. 16, no. 1, pp. 33–40, 2022.

[8] R. S. et al., "Outage probability analysis of selective-decode and forward cooperative wireless network over time varying fading channels with node mobility and imperfect CSI condition," in *TENCON 2018 - 2018 IEEE Region 10 Conference*, Oct 2018, pp. 0508–0513.

[9] M. Bouteggui and F. Merazka, "A joint antenna and path selection for MIMO cooperative communication with single selective decode and forward relay," in *2019 International Conference on Wireless Networks and Mobile Communications (WINCOM)*, 2019, pp. 1–5.

[10] Y. Yao and J. Wen, "SEP performance for selective decode-and-forward cooperative communications over satellite-terrestrial wireless networks," in *2019 International Conference on Intelligent Computing and its Emerging Applications (ICEA)*, 2019, pp. 151–155.

[11] M. Babaei, U. Aygolu, and L. Durak-Ata, "Performance of selective decode-and-forward swipt network in nakagami-M fading channel," in *2018 26th Telecommun. Forum (TELFOR)*, 2018, pp. 1–4.

[12] S. Luo, R. Zhang, and T. J. Lim, "Optimal save-then-transmit protocol for energy harvesting wireless transmitters," *IEEE Trans. Wireless Commun.*, vol. 12, no. 3, pp. 1196–1207, 2013.

[13] C. Chun, J. Kang, and I. Kim, "Adaptive rate and energy harvesting interval control based on reinforcement learning for SWIPT," *IEEE Commun. Letters*, vol. 22, no. 12, pp. 2571–2574, Dec 2018.

[14] M. Abedi, H. Masoumi, and M. J. Emadi, "Power splitting-based SWIPT systems with decoding cost," *IEEE Wireless Commun. Letters*, vol. 8, no. 2, pp. 432–435, April 2019.

[15] C. Liu, M. Maso, S. Lakshminarayana, C. Lee, and T. Q. S. Quek, "Simultaneous wireless information and power transfer under different CSI acquisition schemes," *IEEE Trans. Wireless Commun.*, vol. 14, no. 4, pp. 1911–1926, April 2015.

[16] M. C. G. Zhang, Q. Wu and R. Zhang, "Securing UAV communications via joint trajectory and power control," *IEEE Trans. Wireless Commun.*, vol. 18, no. 2, p. 1376ÍC1389, 2019.

[17] S. X. Wu, W. Ma, and A. M. So, "Physical-layer multicasting by stochastic transmit beamforming and alamouti space-time coding," *IEEE Trans. Signal Processing*, vol. 61, no. 17, pp. 4230–4245, 2013.